ELSEVIER

Journal of Molecular Catalysis A: Chemical 152 (2000) 55–68

JOURNAL OF MOLECULAR CATALYSIS A: CHEMICAL

www.elsevier.com/locate/molcata

Multicenter active sites of vanadium-substituted polyoxometalate catalysts on benzene hydroxylation with hydrogen peroxide and two reaction types with and without an induction period

Kenji Nomiya *, Yukihiro Nemoto, Takeshi Hasegawa, Shin Matsuoka

Department of Materials Science, Kanagawa University, Hiratsuka, Kanagawa 259-1293, Japan

Received 23 April 1999; received in revised form 2 July 1999; accepted 5 July 1999

Abstract

Benzene hydroxylation with hydrogen peroxide catalyzed by selectively site-substituted vanadium (V) polyoxometalates was classified into two reaction types based on the turnover vs. time curve with or without an induction period. A prototypic example was the catalysis by the two geometrical isomers of trivanadium-substituted Keggin-type polyoxotungstate; $[\alpha\text{-}1,2,3\text{-}SiW_9V_3O_{40}]^{7-}$ with a longer induction period and $[\beta\text{-}1,2,3\text{-}SiW_9V_3O_{40}]^{7-}$ without an induction period, respectively. The ^{51}V NMR measurements showed that the former reaction was catalyzed by the vanadium species within the polyoxotungstate, whereas the latter was catalyzed by the vanadium species generated from the polyoxotungstate. This was the case for the catalysis by the previously reported polyoxometalates, i.e., $[\alpha\text{-}1,2,3\text{-}PW_9V_3O_{40}]^{6-}$, $[\alpha\text{-}1,2\text{-}PW_{10}V_2O_{40}]^{5-}$ and $[\alpha\text{-}PMo_{11}VO_{40}]^{4-}$. Also reported are the effect of the countercation on the catalysis by $[\alpha\text{-}1,2\text{-}PW_{10}V_2O_{40}]^{5-}$ and $[\alpha\text{-}PMo_{11}VO_{40}]^{4-}$, and the effect of the used amounts of hydrogen peroxide. The reactions by the Keggin-type $[\alpha\text{-}1,4,9\text{-}PW_9V_3O_{40}]^{6-}$, the two Dawson-type $[\alpha_2\text{-}1,2\text{-}P_2W_{16}V_2O_{62}]^{8-}$ and $[\alpha_2\text{-}P_2W_{15}Mo_2VO_{62}]^{7-}$ polyoxometalates showed turnover vs. time curves without an induction period. However, the ^{31}P and ^{51}V NMR spectra revealed that the reaction by $[\alpha_2\text{-}P_2W_{15}Mo_2VO_{62}]^{7-}$ was catalyzed by the vanadium species within the polyoxometalates. As a model of the catalysis by oxovanadium species generated from polyoxometalates, the reactions using $NaVO_3$ or Na_3VO_4 in water with varied pH were examined. Under the acidic conditions there was no induction period, while under the neutral conditions there was a distinct induction period. The ^{51}V NMR measurements showed that the reactive species participating in these two reactions were $VO(O_2)^+$ and $VO(O_2)_2^-$, respectively.

Keywords: Hydroxylation; Benzene; Vanadium-substituted polyoxometalate; Catalyst precursor; Induction period

1. Introduction

There is currently considerable interest in exploiting both the well-defined structure of the catalyst precursor and the multicenter active site to facilitate the catalysis by polyoxometalates [1–3]. It has been stressed that it is important to

* Corresponding author. Fax: +81-463-58-9684; E-mail: nomiya@info.kanagawa-u.ac.jp

1381-1169/00/$ - see front matter
PII: S1381-1169(99)00283-6

discover more reliable and efficient procedures before exploration of possible new reactivity patterns [4]. Thus, it is very important to use fully characterized and more reliable catalyst precursors for the catalytic reactions.

Catalytic hydroxylation of benzene is a very intriguing reaction by such catalyses. In this reaction, the vanadium (V) center in the polyoxometalates is the key factor, but a coordination environment around it is essential. In fact, we have shown that the di-vanadium substituted Keggin-type polyoxotungstate, $K_5[\alpha\text{-}1,2\text{-}PW_{10}V_2O_{40}]\cdot 4H_2O$ is the most noteworthy catalyst precursor tested in terms of stability and catalytic activity for benzene hydroxylation [5]. An active species for this catalytic reaction has been found to be constructed on the A-site of the Keggin polyoxotungstate, specifically a bimetallic species with corner-shared vanadium octahedra. Furthermore, it has been found that the monovanadium substituted Keggin-type polyoxomolybdate, $(Bu_4N)_4[\alpha\text{-}PMo_{11}VO_{40}]$ also shows the catalytic activity for this reaction. In the latter case, it is likely that a cooperative action of one vanadium center with one of the molybdenum atoms constituting the Keggin skeleton contributes to its catalysis [6], that is, the molybdenum atom adjacent to the vanadium center can substitute a role of the second vanadium atom in the $[\alpha\text{-}1,2\text{-}PW_{10}V_2O_{40}]^{5-}$. In the catalysis by these two polyoxometalates, the turnover vs. time curve showed a longer-time induction period and their activities were relatively low.

In our continuing work, we have been interested in the features of an induction period, which may explain what the oxovanadium species participating in this reaction are. In relation to the induction period in the turnover vs. time curve of benzene hydroxylation, we have unexpectedly found a prototypic example of the catalysis by the potassium salts of two closely related trivanadium-substituted polyoxotungstates, $[\alpha\text{-}1,2,3\text{-}SiW_9V_3O_{40}]^{7-}$ [7] and $[\beta\text{-}1,2,3\text{-}SiW_9V_3O_{40}]^{7-}$ [8], which shows and does not show the induction period, respectively. The ^{51}V NMR measurements of the reaction solutions and also of the solutions containing hydrogen peroxide and the polyoxotungstates without benzene have shown that the reaction with an induction period proceeds on the vanadium species within the polyoxotungstate, but the reaction without an induction period proceeds on the free vanadium species generated from the polyoxotungstate.

Thus, we have further examined benzene hydroxylation catalyzed by the previously reported several polyoxometalates, i.e., $[\alpha\text{-}1,2,3\text{-}PW_9V_3O_{40}]^{6-}$ [7,9], $[\alpha\text{-}1,2\text{-}PW_{10}V_2O_{40}]^{5-}$ [7,9], $[\alpha\text{-}PMo_{11}VO_{40}]^{4-}$ [6], $[\alpha\text{-}PW_{11}VO_{40}]^{4-}$ [7,9], $[\alpha_2\text{-}P_2W_{17}VO_{62}]^{7-}$ [10] and $[\alpha_2\text{-}1,2,3\text{-}P_2W_{15}V_3O_{62}]^{9-}$ [10,11], from the following viewpoints: (1) ^{51}V and ^{31}P NMR measurements of the reaction solutions, (2) an effect of the countercation, Bu_4N or alkali metal, on the turnover vs. time curves of benzene hydroxylation by the two polyoxometalates, $[\alpha\text{-}1,2\text{-}PW_{10}V_2O_{40}]^{5-}$ and $[\alpha\text{-}PMo_{11}VO_{40}]^{4-}$, and ^{51}V and ^{31}P NMR measurements of their reaction solutions, and (3) an effect of the used amounts of hydrogen peroxide on benzene hydroxylation by the two polyoxometalates, $[\alpha\text{-}1,2\text{-}PW_{10}V_2O_{40}]^{5-}$ and $[\alpha\text{-}PMo_{11}VO_{40}]^{4-}$. Further, (4) as a model of the benzene hydroxylation with hydrogen peroxide catalyzed by oxovanadium species generated from polyoxometalates, the catalysis by the oxovanadium species in an aqueous solution, which was prepared by dissolving $NaVO_3$ or Na_3VO_4 in water with varied pH, was examined. (5) Also, examined were the catalysis by the Keggin-type $[\alpha\text{-}1,4,9\text{-}PW_9V_3O_{40}]^{6-}$ [12] and two Dawson-type $[\alpha_2\text{-}1,2\text{-}P_2W_{16}V_2O_{62}]^{8-}$ [10, 13] and $[\alpha_2\text{-}P_2W_{15}Mo_2VO_{62}]^{7-}$ [13] polyoxometalates, and the ^{51}V and ^{31}P NMR characterization of the reaction solutions.

Here, we report the full details of benzene hydroxylation with hydrogen peroxide catalyzed by several selectively vanadium-substituted polyoxometalates and their catalytic turnover vs. time curves. The polyhedral representation of the catalyst precursors used here are shown in the respective figures.

2. Experimental

2.1. Materials

The following were used as received: KCl, NaCl, LiCl, $Na_2WO_4 \cdot 2H_2O$, Li_2MoO_4, $Na_2SiO_3 \cdot 9H_2O$, $VOSO_4 \cdot nH_2O$, AcOH, AcONa $\cdot 3H_2O$, Bu_4NBr, $Na_2HPO_4 \cdot 2H_2O$, $Na_2MoO_4 \cdot 2H_2O$, Li_2CO_3, $KHCO_3$, $NaClO_4$, 12 M aqueous HCl, 6.0 M aqueous HCl, 1.0 M aqueous HCl, 85% H_3PO_4, benzene, 30% aqueous H_2O_2, CH_3CN, EtOH, MeOH, diethyl ether (all from Wako); $NaVO_3$ (Nacalai Tesque); Br_2, AcOK (Kanto); D_2O, DMSO-d_6 (Isotec).

2.2. Apparatus and instrumentation

Infrared (IR) spectra were recorded on a Jasco 300 FT-IR spectrometer in KBr disks at room temperature. Thermogravimetric (TG) and differential thermal analyses (DTA) were acquired using a Rigaku TG8101D and TAS 300 data-processing system. TG/DTA measurements were run under air with a temperature ramp of 4°C per min between 20 and 500°C.

^{31}P NMR (161.70 MHz) and ^{51}V NMR (104.95 MHz) were recorded at 25°C in 5-mm o.d. tubes on a JEOL JNM-EX 400 FT-NMR spectrometer and JEOL EX-400 NMR data-processing system. ^{31}P NMR spectra were referenced to an external standard of 25% H_3PO_4 in H_2O in a sealed capillary and the ^{51}V NMR spectra referenced to an external standard of $VOCl_3$ by a substitution method. The chemical shifts were reported on the δ scale with resonances upfield of H_3PO_4 ($\delta = 0$) as negative and with resonances upfield of $VOCl_3$ ($\delta = 0$) as negative, respectively.

^{183}W NMR (16.50 MHz) spectra were recorded at 25°C in 10-mm o.d. tubes on a JEOL JNM-EX 400 FT-NMR spectrometer equipped with a JEOL NM-40T10L low-frequency tunable probe and JEOL EX-400 NMR data-processing system. ^{183}W NMR spectra were measured in D_2O and referenced to an external standard of saturated Na_2WO_4–D_2O solution by the substitution method. Chemical shifts were reported on the δ scale with resonances upfield of Na_2WO_4 ($\delta = 0$) as negative.

^{29}Si NMR (79.30 MHz) spectra were recorded at 25°C in 5-mm o.d. quartz glass tubes for ^{29}Si NMR measurements on a JEOL JNM-EX 400 FT-NMR spectrometer. These spectra were measured in D_2O solution with reference to an external standard of DSS in D_2O solution, and in DMSO-d_6 solution with reference to an internal standard of TMS. Chemical shifts were reported on the δ scale with resonances upfield of DSS or TMS ($\delta = 0$) as negative.

Gas chromatographic (GC) measurements were carried out on a Shimadzu GC-8APT which was equipped with an Apiezon grease L glass column (Apiezon grease L 10% on Chromosorb W; column length: 2 m; column temperature: 150°C).

2.3. Preparation and characterization of catalyst precursors of polyoxometalates

The following polyoxometalates as catalyst precursors were prepared according to the literature, and their structures were confirmed. Yields and characterization by FT-IR, TG/DTA, ^{31}P, ^{51}V and ^{29}Si NMR, and sometimes by ^{183}W NMR are described below.

$K_4[PW_{11}VO_{40}] \cdot 6H_2O$ [7,9] was obtained in 1.1 g (20.6%) yield. TG/DTA data: 3.6% weight loss was observed below 500°C with an endothermic peak at 73.3°C; calc. for $K_4[PW_{11}VO_{40}] \cdot xH_2O$, 3.6–4.2% ($x = 6$–$7$). ^{31}P NMR ($D_2O$, at room temperature): δ −14.6 ppm. ^{51}V NMR (D_2O, at room temperature): δ −557.8 ppm. Prominent IR bands (KBr disk): 1099 m, 1077 m, 983 m, 883 m, 790 s cm^{-1}.

$K_5[\alpha\text{-}1,2\text{-}PW_{10}V_2O_{40}] \cdot 4H_2O$ [7,9] was obtained in 1.1 g (64.6%) yield. TG/DTA data: 2.7% weight loss was observed below 499°C with an endothermic peak at 69.4°C; calc. for $K_5[\alpha\text{-}1,2\text{-}PW_{10}V_2O_{40}] \cdot xH_2O$, 2.5–3.1% ($x = 4$–$5$). ^{31}P NMR ($D_2O$, at room temperature): δ −14.0 ppm. ^{51}V NMR (D_2O, at room tempera-

ture): δ −549.4 ppm. Prominent IR bands (KBr disk): 1096 m, 1077 m, 1060 m, 963 s, 889 s, 787 s cm^{-1}. $(Bu_4N)_4K[\alpha\text{-}1,2\text{-}PW_{10}V_2O_{40}]$ was obtained in 0.45 g (41.4%) yield. ^{31}P NMR (DMSO-d_6, at room temperature): δ −14.0 ppm. ^{51}V NMR (DMSO-d_6, at room temperature): δ −550.7 ppm. Prominent IR bands (KBr disk): 1097 m, 1077 m, 1061 m, 960 s, 889 s, 805 s, br cm^{-1}.

$K_6[\alpha\text{-}1,2,3\text{-}PW_9V_3O_{40}]\cdot 5H_2O$ [7,9] was obtained in 1.4 g (46.7%) yield. TG/DTA data: 3.2% weight loss was observed below 489°C with an endothermic peak at 48°C; calc. for $K_6[\alpha\text{-}1,2,3\text{-}PW_9V_3O_{40}]\cdot xH_2O$, 3.2–3.8% ($x$ = 5–6). ^{31}P NMR (D_2O, at room temperature): δ −13.8 ppm. ^{51}V NMR (D_2O, at room temperature): δ −570.0 ppm. Prominent IR bands (KBr disk): 1084 m, 1053 m, 964 s, 885 m, 799 s cm^{-1}.

$K_6[\alpha\text{-}1,4,9\text{-}PW_9V_3O_{40}]\cdot 10H_2O$ [12] was obtained in 2.3 g (12.8%) yield. TG/DTA data: 6.11% weight loss was observed below 500°C with an endothermic peak at 68.5°C; calc. for $K_6[\alpha\text{-}1,4,9\text{-}PW_9V_3O_{40}]\cdot xH_2O$, 6.0–6.5% ($x$ = 10–11). ^{31}P NMR (D_2O, pD = 4.0, at room temperature): δ −12.5 ppm. ^{51}V NMR (D_2O, pD = 4.0, at room temperature): δ −503.2 ppm. ^{183}W NMR (D_2O, at room temperature): δ -103.3 (1W), −119.5 (2W) ppm. Prominent IR bands (KBr disk): 1126 m, 1050 m, sh, 956 s, 876 s, 786 s cm^{-1}.

$K_6H[A\text{-}\alpha\text{-}1,2,3\text{-}SiW_9V_3O_{40}]\cdot 11H_2O$ [7] was obtained in 10.8 g (22.8%) yield. TG/DTA data: 6.7% weight loss was observed below 500°C with an endothermic peak at 156.6°C; calc. for $K_6H[A\text{-}\alpha\text{-}1,2,3\text{-}SiW_9V_3O_{40}]\cdot xH_2O$, 6.2–6.8% ($x$ = 10–11). ^{29}Si NMR (D_2O, at room temperature): δ −84.2 ppm. ^{51}V NMR (D_2O, at room temperature): δ −538.1 ppm ($\Delta\nu_{1/2}$ = 413.8 Hz). ^{183}W NMR (D_2O, at room temperature): δ −89.4 (2W), −139.1 (1W) ppm. Prominent IR bands (KBr disk): 1005 m, 918 s, 792 s, 697 m cm^{-1}.

$K_6H[A\text{-}\beta\text{-}1,2,3\text{-}SiW_9V_3O_{40}]\cdot 6H_2O$ [8] was obtained in 10.6 g (19.1%) yield. TG/DTA data: 3.9% weight loss was observed below 500°C with an endothermic peak at 64.3°C; calc. for $K_6H[A\text{-}\beta\text{-}1,2,3\text{-}SiW_9V_3O_{40}]\cdot xH_2O$, 3.8–4.4% ($x$ = 6–7). ^{29}Si NMR (D_2O, at room temperature): δ −84.3 ppm. ^{51}V NMR (D_2O, at room temperature): δ −577.2 ppm ($\Delta\nu_{1/2}$ = 516.4 Hz). ^{183}W NMR (D_2O, at room temperature): δ −114.4 (1W), −115.2 (2W) ppm. Prominent IR bands (KBr disk): 1003 w, 958 m, 905 s, 797 s cm^{-1}.

$K_7[\alpha_2\text{-}P_2W_{17}VO_{62}]\cdot 4H_2O$ [10] was obtained in 1.9 g (64.9%) yield. ^{31}P NMR (D_2O, at room temperature): δ −11.2, −13.3 ppm. ^{51}V NMR (D_2O, at room temperature): δ −557.7 ppm. Prominent IR bands (KBr disk): 1088 s, 956 s, 919 s, 789 s, br cm^{-1}.

$K_8[\alpha_2\text{-}1,2\text{-}P_2W_{16}V_2O_{62}]\cdot 9H_2O$ [10,13] was obtained in 7.0 g (15.3%) yield. TG/DTA data: 3.36% weight loss was observed below 500°C with an endothermic peak at 75.5°C; calc. for $K_8[\alpha_2\text{-}1,2\text{-}P_2W_{16}V_2O_{62}]\cdot xH_2O$, 3.2–3.5% ($x$ = 8–9). ^{31}P NMR (D_2O, at room temperature): δ [major] −9.1, −13.7, [minor] −14.1 ppm. ^{51}V NMR (D_2O, at room temperature): δ [major] −531.3, [minor] −504.6 ppm. Prominent IR bands (KBr disk): 1614 m, 1082 s, 943 s, 917 s, 781 s cm^{-1}.

$K_8H[\alpha_2\text{-}1,2,3\text{-}P_2W_{15}V_3O_{62}]\cdot 17H_2O$ [10,11] was obtained in 17.7 g (74.5%) yield. TG/DTA data: 6.8% weight loss was observed below 499°C with an endothermic peak at 84.5°C; calc. for $K_8H[\alpha_2\text{-}1,2,3\text{-}P_2W_{15}V_3O_{62}]\cdot xH_2O$, 6.7–7.0% ($x$ = 17–18). ^{31}P NMR (D_2O, at 70°C): δ −6.3, −13.9 ppm. ^{51}V NMR (D_2O, at room temperature): δ −517.0 ppm. Prominent IR bands (KBr disk): 1080 s, 1048 m, 1013 w, 937 s, 881 m, 773 s, br cm^{-1}.

$K_7[\alpha_2\text{-}1,2,3\text{-}P_2W_{15}Mo_2VO_{62}]\cdot 13H_2O$ [13] was obtained in 7.0 g (15.2%) yield. TG/DTA data: 5.0% weight loss was observed below 499°C with an endothermic peak at 74.3°C; calc. for $K_7[\alpha_2\text{-}1,2,3\text{-}P_2W_{15}Mo_2VO_{62}]\cdot xH_2O$, 4.8–5.1% ($x$ = 12–13). ^{31}P NMR (D_2O, at room temperature): δ −11.2, −13.3 ppm. ^{51}V NMR (D_2O, at room temperature): δ −558.0 ppm. Prominent IR bands (KBr disk): 1086 w, 954 s, 917 s, 786 s cm^{-1}.

$(Bu_4N)_4[\alpha\text{-}PMo_{11}VO_{40}]$ [6] was obtained in 11.6 g (42.2%) yield. TG/DTA data: no weight loss was observed below 286°C. An exothermic peak due to decomposition was observed at 302°C. ^{31}P NMR (DMSO-d_6, at room temperature): δ −3.8 ppm. ^{51}V NMR (DMSO-d_6, at room temperature): δ −526.8 ppm. Prominent IR bands (KBr disk): 1077 m, 1056 m, 941 s, 872 m, 801 s cm^{-1}. $K_4[\alpha\text{-}PMo_{11}VO_{40}]\cdot 5H_2O$ was obtained in 2.6 g (66.5%) yield. TG/DTA data: 4.8% weight loss was observed below 499°C with an endothermic peak at 89.5°C; calc. for $K_4[\alpha\text{-}PMo_{11}VO_{40}]\cdot xH_2O$, 4.6–5.3% ($x = 5$–6). ^{31}P NMR (D_2O, at room temperature): δ −3.9 ppm. ^{51}V NMR (D_2O, at room temperature): δ −532.6 ppm. Prominent IR bands (KBr disk): 1062 s, 961 s, 865 s, 781 s cm^{-1}. $Na_4[\alpha\text{-}PMo_{11}VO_{40}]\cdot 8H_2O$ was obtained in 3.8 g (37.6%) yield. TG/DTA data: 7.16% weight loss was observed below 499°C with endothermic peaks at 51.2, 69.8, 108.4, 219.6°C; calc. for $Na_4[\alpha\text{-}PMo_{11}VO_{40}]\cdot xH_2O$, 6.32–7.98% ($x = 7$–9). ^{31}P NMR (D_2O, at room temperature): δ −3.84 ppm. ^{51}V NMR (D_2O, at room temperature): δ −533.9 ppm. Prominent IR bands (KBr disk): 1063 m, 961 s, 867 m, 781 s cm^{-1}.

2.4. Typical oxidation procedures and products analysis

The oxidation reaction of benzene was carried out at 25°C in a 50-ml round-bottom flask. The reaction system consisted of two liquid phases: an organic layer containing benzene and acetonitrile, and an aqueous layer containing acetonitrile and 30% H_2O_2. In a typical experiment, 0.10 mmol of catalyst precursor, 10 ml (113 mmol) of benzene, 2 ml (25.4 mmol) of aqueous 30% H_2O_2, and varied amounts (2, 5 and 10 ml) of acetonitrile in a 50-ml round-bottom flask with a serum cap were employed. A magnetic stirrer was provided to stir the reaction medium. The oxidation reaction at 25°C was monitored at various time intervals by GC analysis (an Apiezon grease L column). For the organic phase in the presence of acetonitrile, 1.5 μl were sampled using a microsyringe and analyzed. The reaction product, phenol, was quantitatively analyzed using the calibration curve based on the relative area of each of authentic samples relative to an acetonitrile. In quantitative analysis of phenol, the amounts contained in the organic layer were actually much more than those in the aqueous layer; the latter amounts were negligible. Catalytic turnovers were estimated as a ratio of product (mmol)/catalyst precursor (mmol).

3. Results and discussion

3.1. Benzene hydroxylation catalyzed by $[\alpha\text{-}1,2,3\text{-}SiW_9V_3O_{40}]^{7-}$ and $[\beta\text{-}1,2,3\text{-}SiW_9V_3O_{40}]^{7-}$

Benzene oxidation with H_2O_2 catalyzed by the water-soluble potassium salts of two polyoxotungstates, $[\alpha\text{-}1,2,3\text{-}SiW_9V_3O_{40}]^{7-}$ and $[\beta\text{-}1,2,3\text{-}SiW_9V_3O_{40}]^{7-}$ to produce phenol results in a quite different, but noteworthy turnover vs. time curve (Fig. 1). Although both reactions proceed catalytically, their reactivity patterns are quite different. The reaction by $[\alpha\text{-}1,2,3\text{-}SiW_9V_3O_{40}]^{7-}$ shows an induction period and its curve shape is downwards convex, while that by $[\beta\text{-}1,2,3\text{-}SiW_9V_3O_{40}]^{7-}$ shows no induction period and the curve shape is upwards convex.

The ^{51}V NMR spectra of the reaction solutions and also of the aqueous solution containing the polyoxometalates in the presence of hydrogen peroxide (without benzene) were compared with those of these polyoxotungstates before the reactions. It was found that the polyoxoanion structure of $[\alpha\text{-}1,2,3\text{-}SiW_9V_3O_{40}]^{7-}$ was retained even after 7 days (^{51}V NMR; δ −554.2 ppm [major peak]), whereas that of $[\beta\text{-}1,2,3\text{-}SiW_9V_3O_{40}]^{7-}$ decomposed completely before 48 h (only one ^{51}V NMR signal; δ −524.2 ppm). The solid-state FT-IR spectra of the samples recovered after the reactions also supported these facts. Thus, the reaction by the $[\alpha\text{-}1,2,3\text{-}SiW_9V_3O_{40}]^{7-}$ is promoted by the

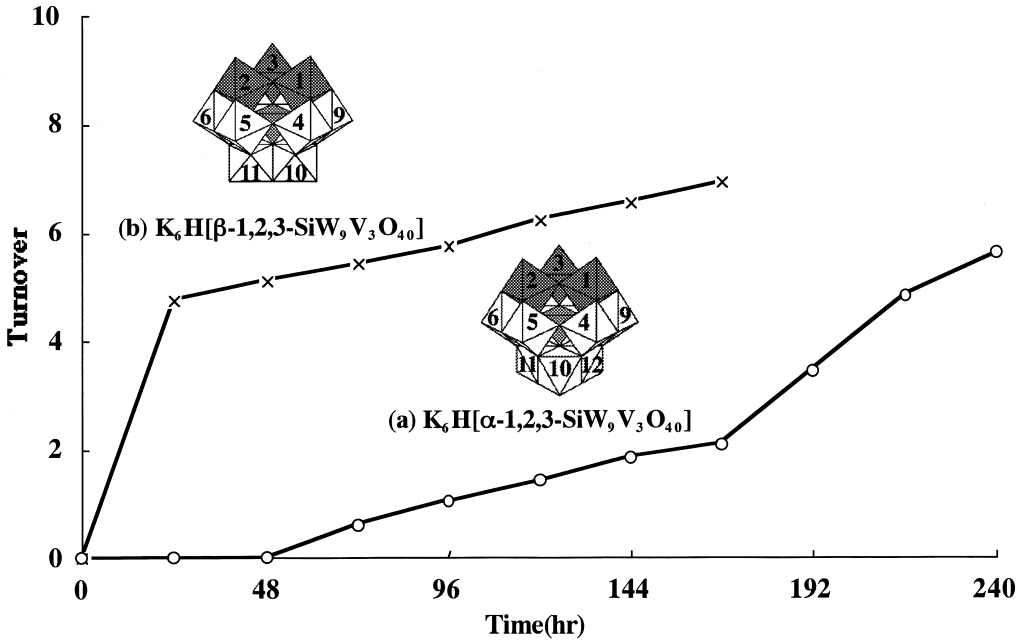

Fig. 1. Benzene oxidation with hydrogen peroxide catalyzed by two closely related polyoxotungstates, (a) $K_6H[\alpha\text{-}1,2,3\text{-}SiW_9V_3O_{40}]$ and (b) $K_6H[\beta\text{-}1,2,3\text{-}SiW_9V_3O_{40}]$ under the conditions: 0.1 mmol catalyst precursors, 2 ml (25.4 mmol) of 30% H_2O_2, 10 ml (111.5 mmol) benzene and 5 ml of CH_3CN at room temperature.

vanadium species within this polyoxotungstate, while that by the $[\beta\text{-}1,2,3\text{-}SiW_9V_3O_{40}]^{7-}$ is promoted by the vanadium species generated from the polyoxotungstate. Probably it takes longer to form the reactive species between the vanadium species within the $[\alpha\text{-}1,2,3\text{-}SiW_9V_3O_{40}]^{7-}$ and hydrogen peroxide, resulting in the longer induction period. On the contrary, the vanadium species, which showed ^{51}V NMR signal at δ −524.2 ppm, generated from the reaction of $[\beta\text{-}1,2,3\text{-}SiW_9V_3O_{40}]^{7-}$ with hydrogen peroxide will readily form the reactive species, and, therefore, the catalytic reaction will proceed without an induction period. These are also suggested by a model reaction using an oxovanadium species and hydrogen peroxide [see Section 3.7].

Thus, Fig. 1 is a prototypic example, indicating that in the reactions by two closely related polyoxotungstates, the species participating in the reaction are quite different, and also suggesting that the reaction with an induction period proceeds on the vanadium species within the polyoxotungstate, while the reaction without an induction period proceeds on the vanadium species out of the polyoxotungstate.

3.2. Previously reported benzene hydroxylation catalyzed by $[\alpha\text{-}1,2,3\text{-}PW_9V_3O_{40}]^{6-}$ and $[\alpha\text{-}1,2\text{-}PW_{10}V_2O_{40}]^{5-}$

The previously reported reactions [5] catalyzed by the water-soluble potassium salts of two polyoxotungstates, $[\alpha\text{-}1,2,3\text{-}PW_9V_3O_{40}]^{6-}$ and $[\alpha\text{-}1,2\text{-}PW_{10}V_2O_{40}]^{5-}$ also show the turnover vs. time curves without and with the induction period, respectively (Fig. 2). In fact, the $[\alpha\text{-}1,2,3\text{-}PW_9V_3O_{40}]^{6-}$ readily reacts with H_2O_2 to produce free oxovanadium ions and its original polyoxoanion structure is not retained. [1] On the other hand, the reaction by $[\alpha\text{-}1,2\text{-}PW_{10}V_2O_{40}]^{5-}$ proceeds on the oxovanadium

[1] It should decompose much faster than 48 h (time), which was previously described [5].

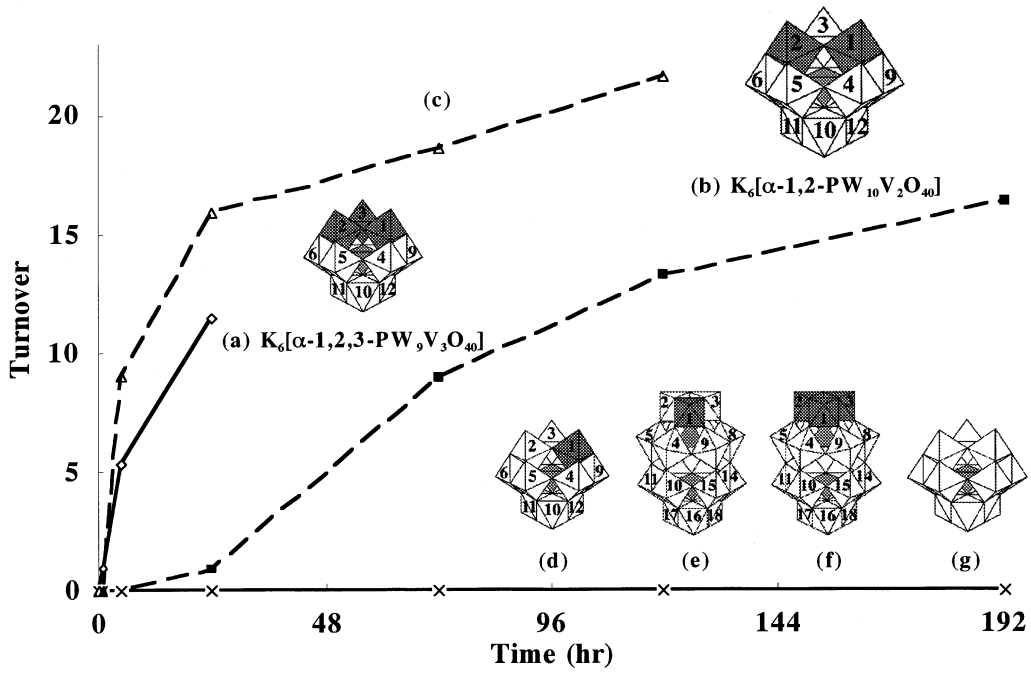

Fig. 2. Benzene oxidation with hydrogen peroxide catalyzed by two polyoxotungstates, (a) $K_6[\alpha\text{-}1,2,3\text{-}PW_9V_3O_{40}]$ and (b) $K_5[\alpha\text{-}1,2\text{-}PW_{10}V_2O_{40}]$ under the conditions: 0.1 mmol catalyst precursors, 2 ml (25.4 mmol) of 30% H_2O_2, 10 ml (111.5 mmol) benzene and 2 ml of CH_3CN at room temperature. The curve (c) results from the second reaction using the $[PW_{10}V_2O_{40}]^{5-}$ recovered after 144-h reaction in (b). The recovery of the sample in the first reaction is based on evaporation to dryness, washing with ether and then collection of a water-soluble species. The catalyst precursors (d) $[\alpha\text{-}PW_{11}VO_{40}]^{4-}$, (e) $[\alpha_2\text{-}P_2W_{17}VO_{62}]^{7-}$ and (f) $[\alpha_2\text{-}1,2,3\text{-}P_2W_{15}V_3O_{62}]^{9-}$, as well as the parent polyoxometalates (g) $[\alpha\text{-}PM_{12}O_{40}]^{3-}$ (M = Mo, W), did not show any activities for benzene oxidation [4,5].

species within this polyoxotungstate and the original structure is retained for a relatively longer time.

The ^{31}P and ^{51}V NMR measurements of the 48- and 144-h reaction solutions of the $K_5[\alpha\text{-}1,2\text{-}PW_{10}V_2O_{40}]$ revealed that this polyoxotungstate retained its original structure up to 48 h, but more than a half of its structure decomposed after 144-h reaction. [2] In fact, the second reaction using the sample, recovered by collecting the water-soluble species from evaporation to dryness of the aqueous layer after 144-h reaction and then washing with ether, showed the upwards convex curve without an induction period (Fig. 2c). Thus, the turnover vs. time curves with and without an induction period suggest that an early stage of the first reaction by the $K_5[\alpha\text{-}1,2\text{-}PW_{10}V_2O_{40}]$ is promoted by the vanadium species within the polyoxotungstate, while the second reaction by the recovered sample is promoted by the vanadium species generated from the polyoxotungstate.

As previously described [5], the catalyst precursors $[\alpha\text{-}PW_{11}VO_{40}]^{4-}$, $[\alpha_2\text{-}P_2W_{17}VO_{62}]^{7-}$ and $[\alpha_2\text{-}1,2,3\text{-}P_2W_{15}V_3O_{62}]^{9-}$, as well as the parent polyoxometalates $[\alpha\text{-}PW_{12}O_{40}]^{3-}$ and $[\alpha\text{-}PMo_{12}O_{40}]^{3-}$, do not show any activities for benzene oxidation [5] (Fig. 2). Thus, although the benzene oxidation requires the vanadium

[2] It has been previously reported that the ^{51}V NMR measured after the 576-h reaction exhibited the preserved Keggin polyoxoanion structure [5]. However, during a longer course of reaction, the original ^{31}P and ^{51}V NMR signals disappear, and, instead, many signals appear. For example, the ^{31}P NMR of the solution after 144-h reaction showed major peaks at −13.9 and −14.5 ppm and minor peaks at −13.7 and −14.0 ppm, and the ^{51}V NMR showed major peaks at −549.2 and −558.0 ppm and minor peaks at −529.0, −556.4 and −559.9 ppm. Although a complete assignment of these signals is difficult, these NMR behaviors are consistent with the reactivity pattern.

center, the reactive peroxo vanadium species will not be formed for these vanadium-substituted Keggin and Dawson polyoxometalates, neither within the polyoxometalates nor out of the polyoxometalates.

3.3. Effect of the countercation, Bu_4N or alkali metal, on benzene hydroxylation by two polyoxometalates, $[\alpha\text{-}1,2\text{-}PW_{10}V_2O_{40}]^{5-}$ and $[\alpha\text{-}PMo_{11}VO_{40}]^{4-}$

In the reaction system, the water-soluble alkali metal salt of the polyoxometalate is dissolved in the lower aqueous layer containing hydrogen peroxide, while the CH_3CN-soluble Bu_4N salt is dissolved in the upper organic layer containing benzene. Fig. 3c shows that the turnover vs. time curve by the BuN_4 salt of $[\alpha\text{-}1,2\text{-}PW_{10}V_2O_{40}]^{5-}$ is accompanied with an induction period of about 24 h, suggesting the reaction proceeds on the vanadium species within the polyoxotungstate. However, it should be noted that the stability as catalyst was markedly different in the potassium and Bu_4N salts of $[\alpha\text{-}1,2\text{-}PW_{10}V_2O_{40}]^{5-}$; the potassium salt has shown that only an early stage of the first reaction proceeds with its polyoxoanion structure intact retained, but the second reaction using the recovered sample after the first reaction does not [see Section 3.2, and Fig. 2b and 2c]. On the contrary, as shown in Fig. 3d, the Bu_4N salt showed that the second reaction by the recovered sample also proceeded with its structure intact retained. The stability as catalyst of the Bu_4N salt was also confirmed by the ^{31}P and ^{51}V NMR measurements of the recovered sample after the first reaction.

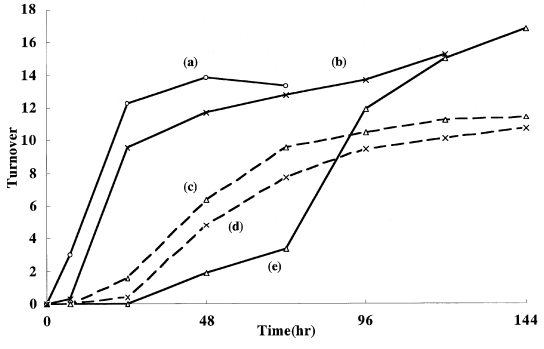

Fig. 3. Effect of the countercation, Bu_4N or alkali metal, on benzene hydroxylation by two polyoxometalates, $[\alpha\text{-}1,2\text{-}PW_{10}V_2O_{40}]^{5-}$ and $[\alpha\text{-}PMo_{11}VO_{40}]^{4-}$. The turnover vs. time curves were obtained by (a) $Na_4[\alpha\text{-}PMo_{11}VO_{40}]$, (b) $K_4[\alpha\text{-}PMo_{11}VO_{40}]$, (c) $(Bu_4N)_4K[\alpha\text{-}1,2\text{-}PW_{10}V_2O_{40}]$ and (e) $(Bu_4N)_4[\alpha\text{-}PMo_{11}VO_{40}]$ under the conditions: 0.1 mmol catalyst precursors, 2 ml (25.4 mmol) of 30% H_2O_2, 10 ml (111.5 mmol) benzene, and 5 ml (for (a) and (b)) and 10 ml (for (c) and (e)) of CH_3CN at room temperature. The curve (d) results from the second reaction under the conditions of 0.05 mmol catalyst precursor, 1 ml of 30% H_2O_2, 5 ml benzene and 5 ml CH_3CN at room temperature using the $(Bu_4N)_4K[\alpha\text{-}1,2\text{-}PW_{10}V_2O_{40}]$ recovered after 7 days' reaction in (c). The recovery of the sample from the first reaction was performed by evaporating the organic layer, collecting the powder and washing with ether and then water.

Similar trends were observed in the catalysis by $[\alpha\text{-}PMo_{11}VO_{40}]^{4-}$. The turnover vs. time curve by its water-soluble sodium salt is upwards convex without a distinct induction period (Fig. 3a), which is in contrast to that by the Bu_4N salt [6] showing downwards convex with an induction period of 24 h (Fig. 3e). Although the curve by the water-soluble potassium salt of $[\alpha\text{-}PMo_{11}VO_{40}]^{4-}$ shows a very short induction period of 7 h (Fig. 3b), its shape is similar to that by the sodium salt, rather than that by the Bu_4N salt.

Thus, the catalysis by $[\alpha\text{-}1,2\text{-}PW_{10}V_2O_{40}]^{5-}$ and $[\alpha\text{-}PMo_{11}VO_{40}]^{4-}$, and their stability as catalysts are strongly dependent on the countercation, Bu_4N or alkali metal.

The remarkable stability of the Bu_4N salt of $[\alpha\text{-}PMo_{11}VO_{40}]^{4-}$ and the instability of the sodium salt were confirmed by the ^{31}P and ^{51}V NMR measurements and also by the second reactions by the recovered samples after the first reactions. The Bu_4N salt of $[\alpha\text{-}PMo_{11}VO_{40}]^{4-}$ is stable as a catalyst precursor and, in fact, the second reaction using the recovered sample after 11-days' reaction also showed the downwards convex curve with almost unchanged induction period. The ^{51}V NMR spectra of the reaction solution of the Bu_4N salt showed that the original polyoxoanion structure was retained after 144-h reaction. On the other hand, the ^{51}V

NMR spectra revealed that the sodium salt of $[\alpha\text{-}PMo_{11}VO_{40}]^{4-}$ readily decomposed before 27 h by the reaction with hydrogen peroxide and released a free oxovanadium species, which showed only one ^{51}V NMR peak at -693.2 ppm (this signal is not assignable to the $VO(O_2)_2^-$ species (δ -698 ppm) described in Section 3.7).

3.4. Effect of the used amounts of hydrogen peroxide on benzene hydroxylation by two polyoxometalates, $[\alpha\text{-}1,2\text{-}PW_{10}V_2O_{40}]^{5-}$ and $[\alpha\text{-}PMo_{11}VO_{40}]^{4-}$

Dependence of the amounts of aqueous hydrogen peroxide used on benzene hydroxylation catalyzed by $K_5[\alpha\text{-}1,2\text{-}PW_{10}V_2O_{40}]$ and $(Bu_4N)_4[\alpha\text{-}PMo_{11}VO_{40}]$ is shown in Fig. 4. Both reactions strongly depended on the amounts of hydrogen peroxide, and their induction periods were significantly reduced by the increased concentration of hydrogen peroxide. Of particular note was that the catalytic turnover drastically dropped in the range of less than 15% concentration of hydrogen peroxide. This drop is attributed to the fact that these polyoxometalates also effectively catalyze decomposition of hydrogen peroxide. In fact, since the benzene oxidation catalyzed by these polyoxometalates are also accompanied with decomposition of hydrogen peroxide, i.e., catalase-like reaction, it seems that the catalytic turnover of phenol production after a longer time does not increase. Furthermore, the consumed amounts of hydrogen peroxide are much more than the produced amounts of phenol.

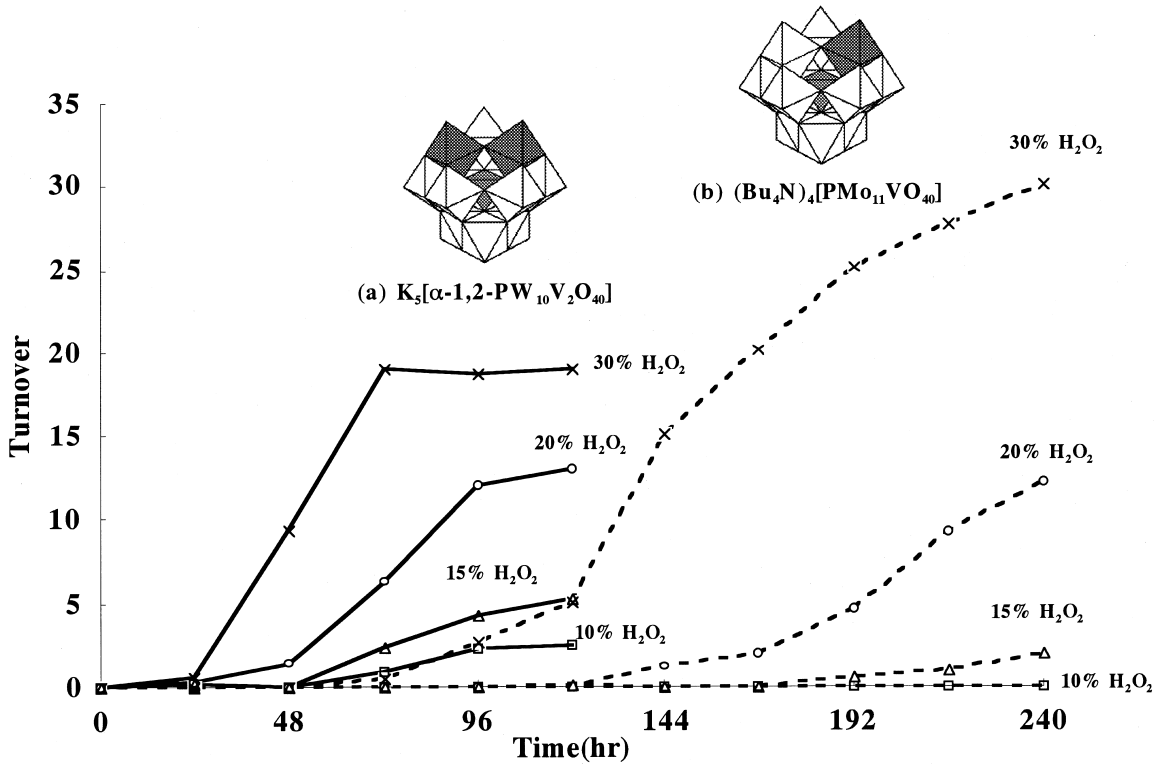

Fig. 4. Dependence of the amounts of hydrogen peroxide used on benzene hydroxylation catalyzed by (a) $K_5[\alpha\text{-}1,2\text{-}PW_{10}V_2O_{40}]$ and (b) $(Bu_4N)_4[\alpha\text{-}PMo_{11}VO_{40}]$ under the conditions: 0.1 mmol catalyst precursors, 4 ml each of 10, 15, 20, 30% H_2O_2, 10 ml (111.5 mmol) benzene and 2 ml (for (a)) and 10 ml (for (b)) of CH_3CN at room temperature.

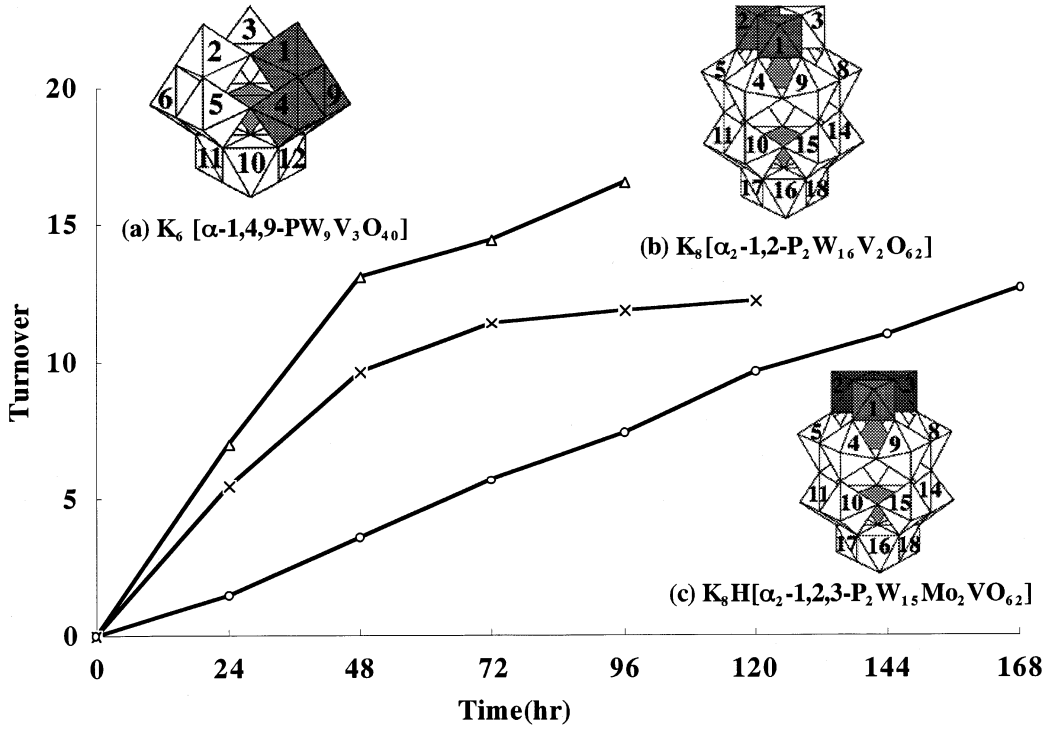

Fig. 5. Benzene oxidation catalyzed by (a) Keggin-type $K_6[\alpha\text{-}1,4,9\text{-}PW_9V_3O_{40}]$, two Dawson-type (b) $K_8[\alpha_2\text{-}1,2\text{-}P_2W_{16}V_2O_{62}]$ and (c) $K_7[\alpha_2\text{-}P_2W_{15}Mo_2VO_{62}]$ polyoxometalates under the conditions: 0.1 mmol catalyst precursors, 2 ml (25.4 mmol) of 30% H_2O_2, 10 ml (111.5 mmol) benzene and 5 ml of CH_3CN at room temperature.

3.5. Benzene hydroxylation catalyzed by Keggin-type $[\alpha\text{-}1,4,9\text{-}PW_9V_3O_{40}]^{6-}$, Dawson-type $[\alpha_2\text{-}1,2\text{-}P_2W_{16}V_2O_{62}]^{8-}$ and $[\alpha_2\text{-}P_2W_{15}Mo_2VO_{62}]^{7-}$

The reactions by Keggin-type $K_6[\alpha\text{-}1,4,9\text{-}PW_9V_3O_{40}]$, Dawson-type $K_8[\alpha_2\text{-}1,2\text{-}P_2W_{16}V_2O_{62}]$ and $K_7[\alpha_2\text{-}P_2W_{15}Mo_2VO_{62}]$ (Fig. 5) show also effective catalysis for benzene hydroxylation with hydrogen peroxide. It should be noted that these reactions are not associated with an induction period. Although the local geometries around the vanadium atoms of $[\alpha\text{-}1,4,9\text{-}PW_9V_3O_{40}]^{6-}$ and $[\alpha_2\text{-}P_2W_{15}Mo_2VO_{62}]^{7-}$ resemble those of $[\alpha_2\text{-}1,2,3\text{-}P_2W_{15}V_3O_{62}]^{9-}$ and $[\alpha\text{-}PMo_{11}O_{40}]^{4-}$, respectively, their catalyses and stabilities as catalysts are not at all similar. Of particular note was the remarkable stability as catalyst of $[\alpha_2\text{-}P_2W_{15}Mo_2VO_{62}]^{7-}$. The ^{31}P and ^{51}V NMR spectra in D_2O of the samples recovered after the reaction showed that the original structures of $[\alpha\text{-}1,4,9\text{-}PW_9V_3O_{40}]^{6-}$ and $[\alpha_2\text{-}1,2P_2\text{-}W_{16}V_2O_{62}]^{8-}$ were not maintained, but that of $[\alpha_2\text{-}P_2W_{15}Mo_2VO_{62}]^{7-}$ was retained even after 11-days' reaction. [3] Although these three polyoxometalates showed the turnover vs. time curves without an induction period (Fig. 5a–5c), it has been suggested that the reaction by the

[3] After the 144-h reaction by the $[\alpha\text{-}1,4,9\text{-}PW_9V_3O_{40}]^{6-}$, the ^{31}P NMR showed major peaks at −11.9 and −13.7 ppm and minor peaks at −13.9 and −14.0 ppm, and the ^{51}V NMR showed major peaks at −522.2 and −529.0 ppm and minor peaks at −556.5 and −560.0 ppm. On the other hand, after 8-days' reaction of the $[\alpha_2\text{-}1,2\text{-}P_2W_{16}V_2O_{62}]^{8-}$, the ^{31}P NMR showed major peaks at −9.2 and −13.7 ppm and minor peaks at −11.1, −11.6, −12.7, −13.2 and −13.8 ppm, and the ^{51}V NMR showed a major peak at −543.5 ppm and a minor peak at −558.1 ppm). After 11-days' reaction by the $[\alpha_2\text{-}P_2W_{15}Mo_2VO_{62}]^{7-}$, the ^{31}P NMR showed major peaks at −11.2 and −13.3 ppm and minor peaks at −10.2 and −13.8 ppm, and the ^{51}V NMR showed only a signal at −557.8 ppm.

$[\alpha_2\text{-}P_2W_{15}Mo_2VO_{62}]^{7-}$ proceeds on the vanadium species within the polyoxometalate, but others do not. In this case the reactive species may be, *exceptionally*, readily formed between hydrogen peroxide and the vanadium species within the polyoxometalate.

3.6. pH dependent distribution of vanadate species present in aqueous solution

Oxoanions of vanadium including orthovanadate (tetraoxovanadate) VO_4^{3-}, metavanadate (trioxovanadate) VO_3^- and heptaoxodivanadate $V_2O_7^{4-}$, generally called vanadate, exist as various oligomeric species in aqueous solution, in equilibrium with one another, and their solution chemistry is exceedingly complex [14]. The species distribution is influenced by the vanadium ion concentration, the buffer composition, the temperature, and the ionic strength of the medium. At vanadate concentration of 1 mM and pH values of >9, the vanadate monomers such as VO_4^{3-}, HVO_4^{2-} and $H_2VO_4^-$ are favored, while near pH 7 the vanadate tetramer is reported to predominate [15,16].

The ^{51}V NMR spectra were measured under varied pH of 0.5 M $NaVO_3$ unbuffered aqueous solution. By comparison with the previously reported ^{51}V NMR analysis based on pH, concentration, equilibrium, chemical shift and $\Delta\nu_{1/2}$ of the solution containing vanadate ion [17,18], it is found that various species are present in the solution; in the pH range of 7.3–6.6, cyclic tetravanadate, $V_4O_{12}^{4-}$, V_4 (-576.7 ppm) is present as a major species and cyclic pentavanadate, $V_5O_{15}^{5-}$, V_5 (-585.2 ppm) as a minor species; in the range of pH <6.0, decavanadate $V_{10}O_{28}^{6-}$, V_{10} (-423.3, -499.6, -515.1 ppm) begins to appear and in the pH range of 4.1–3.0, only V_{10} and its protonated species (-425.3, -505.0, -521.8 ppm; -425.5, -506.7, -524.3 ppm) are present; in the pH 2.0, monomeric VO_2^+ (-545.1 ppm), in addition to V_{10}, appears, and in the range of pH <1 only a VO_2^+ (-544.9 ppm) is present. It has been reported that the VO_2^+ cation has an octahedral *cis*-dioxo structure [18]. Also, measured were the pH dependent ^{51}V NMR spectra of an unbuffered aqueous solution containing 0.5 M Na_3VO_4; in the pH 11, the monomeric, tetrahedral VO_4^{3-} and its protonated species or dimeric $HV_2O_7^{3-}$ (-535.9 and -560 ppm) are present; in the pH 9, V_4 (-576.3 ppm) as a major species and V_5 (-584.6 ppm) as a minor species are present; in the pH 7, V_{10} (-422.9, -498.7, -514.7 ppm) begins to appear in addition to V_4 and V_5 species; in the pH range of 5–3, only a V_{10} species is present; and in the pH 1, only a VO_2^+ (-544.3 ppm) is present.

3.7. Benzene hydroxylation catalyzed by oligomeric and monomeric oxovanadium species; a model of benzene hydroxylation by the vanadium species generated from poyoxotungstates

In the benzene hydroxylation catalyzed by vanadium-substituted polyoxometalates, regardless of the radical or non-radical mechanism, whether the turnover vs. time curve shows an induction period or not has been attributed to the different oxovanadium species participating in this reaction. In order to confirm this fact and also to realize a model reaction by vanadium species generated from polyoxotungstates, we have examined benzene hydroxylation by an aqueous $NaVO_3$ solution and hydrogen peroxide system.

Fig. 6 shows the results of benzene oxidation reaction under the conditions that major V_4 species and minor V_5 species exist predominantly; 0.1 mmol $NaVO_3$, 4 ml of 30% H_2O_2, 10 ml benzene and 5 ml of CH_3CN at room temperature. The reaction proceeds catalytically after an induction period of ca. 24 h; catalytic turnovers were 0.41 at 24-h reaction, 8.36 at 48 h and 21.7 at 72 h (Fig. 6a). In this reaction, the turnover vs. time curve becomes downwards convex. On the other hand, under the pH <1 conditions that only the octahedral VO_2^+ species is present, i.e., (i) 0.1 mmol $NaVO_3$ + 0.1 ml of 1.0 M aqueous HCl and (ii) 0.1 mmol $NaVO_3$

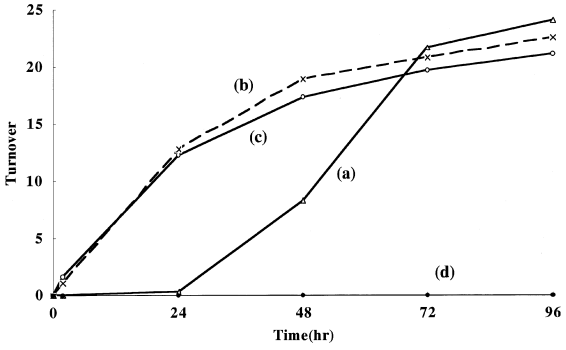

Fig. 6. Benzene oxidation at room temperature under the conditions: (a) 0.1 mmol $NaVO_3$ in which major V_4 and minor V_5 species are present predominantly; (b) 0.1 mmol $NaVO_3$ + 0.1 ml of 1.0 M aqueous HCl and (c) 0.1 mmol $NaVO_3$ + 0.2 ml of 1.0 M aqueous HCl in which only the VO_2^+ species is present; and (d) 0.1 mmol Na_3VO_4 in which monomeric tetrahedral VO_4^{3-} and its protonated species or dimeric $HV_2O_7^{3-}$ are present (pH > 9); in (a)–(d), 4 ml (50.8 mmol) of 30% H_2O_2, 10 ml (111.5 mmol) benzene and 5 ml of CH_3CN were used.

+ 0.2 ml of 1.0 M aqueous HCl, the benzene oxidation starts immediately without an induction period; catalytic turnovers of (i) and (ii) were (1.08, 1.67) at 2-h reaction, (12.8, 12.3) at 24 h, and (19.0, 17.3) at 48 h (Fig. 6b,c). In these reactions, the turnover vs. time curve becomes upwards convex. Furthermore, under the pH > 9 conditions that tetrahedral VO_4^{3-} and its protonated species or dimeric $HV_2O_7^{3-}$ exist predominantly, i.e., 0.1 mmol Na_3VO_4, 4 ml of 30% H_2O_2, 10 ml benzene and 5 ml of CH_3CN at room temperature, no reaction occurred (Fig. 6d).

The ^{51}V NMR spectra of $NaVO_3$ aqueous solution in the presence of hydrogen peroxide showed that the $VO(O_2)_2^-$ species (−697.3 ppm) was exclusively formed at 22 h (Fig. 7b), while the $VO(O_2)^+$ species as a major peak at −543.8 ppm was mainly formed at 27 h (Fig. 7c). In Fig. 7c, three minor peaks at −426.1, −512.2 and −531.9 ppm are probably due to a protonated species of V_{10} and a minor peak at −538.0 ppm is due to a VO_2^+ cation.

The affinity of the VO_2^+ species (V_1) with hydrogen peroxide is very large. In fact, an equilibrium between VO_2^+ and hydrogen peroxide in aqueous solution has been well described by Clague and Butler [19] and the determination of formation constants and the assignment of three peroxides in the ^{51}V NMR spectra have been achieved [19,20];

$$VO_2^+ + H_2O_2 \rightleftarrows VO(O_2)^+ + H_2O \quad (1)$$

$$K_1(3.7\times10^4\,M^{-1});\quad \delta(^{51}V) - 540\,ppm$$

$$VO(O_2)^+ + H_2O_2 \rightleftarrows VO(O_2)_2^- + 2H^+ \quad (2)$$

$$K_2(0.6\pm0.1\,M);\quad \delta(^{51}V) - 698\,ppm$$

$$VO(O_2)^+ + VO(O_2)_2^- \rightleftarrows (VO)_2(O_2)_3 \quad (3)$$

$$K_3(9\,M^{-1}\,\text{at pH}\,0\text{–}2);\quad \delta(^{51}V) - 670\,ppm$$

The $VO(O_2)^+$ species is readily formed under acidic conditions, while the formation of

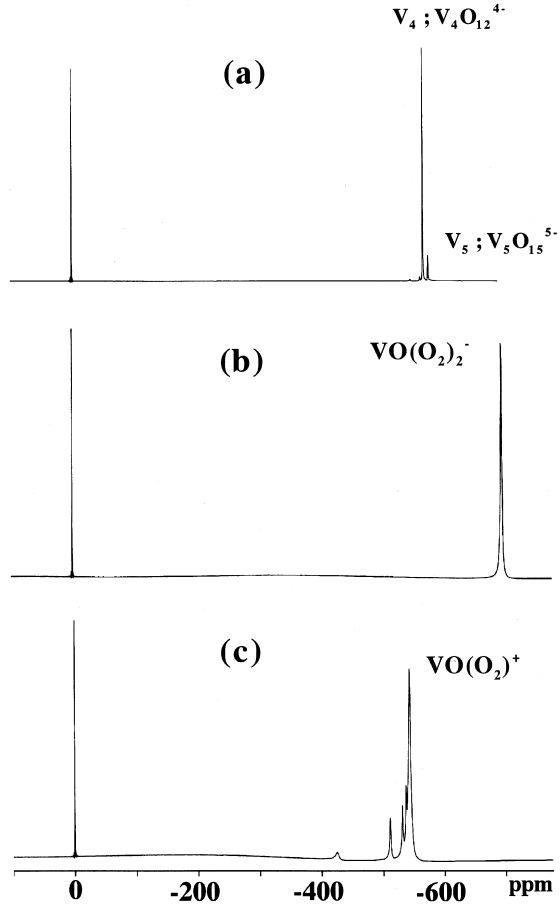

Fig. 7. The ^{51}V NMR spectra of aqueous $NaVO_3$ solution; (a) 0.1 M $NaVO_3$ unbuffered aqueous solution (pH 7.3), (b) after 22 h reaction of the solution containing 0.3 mmol $NaVO_3$ and 6 ml of 30% H_2O_2 and (c) after 27 h reaction of the solution containing 0.1 mmol $NaVO_3$, 0.1 ml of 1 M aqueous HCl and 2 ml of 30% H_2O_2.

$VO(O_2)_2^-$ species from the $VO(O_2)^+$ is not favored under acidic conditions. Thus, in Fig. 6a, either the formation process of the $VO(O_2)_2^-$ species from the reaction between the cyclic oligomers (V_4 and V_5 species) and hydrogen peroxide, or the successive formation of a reactive O^+ or $O\cdot$ species, which may actually attack benzene, from the $VO(O_2)_2^-$ species will be the rate-determining step in the benzene hydroxylation and may account for an induction period.

Hence, the reactions of hydrogen peroxide with the vanadium species within the polyoxometalates may resemble those of the cyclic V_4 and V_5 species with hydrogen peroxide producing the $VO(O_2)_2^-$.

4. Summary

Benzene hydroxylation with hydrogen peroxide catalyzed by various vanadium-substituted polyoxometalates was classified into two reaction types, based on the turnover vs. time curves with or without an induction period. The ^{31}P and ^{51}V NMR measurements have suggested that, generally, the reactions accompanied with an induction period proceed on the vanadium species within the polyoxometalates, while those without an induction period proceed on the vanadium species generated from the polyoxometalates. Prototypic examples were observed; the former example was by $[\alpha\text{-}1,2,3\text{-}SiW_9V_3O_{40}]^{7-}$ and the latter example by $[\beta\text{-}1,2,3\text{-}SiW_9V_3O_{40}]^{7-}$. The turnover vs. time curves by the previously reported vanadium-substituted polyoxometalates such as $[\alpha\text{-}1,2,3\text{-}PW_9V_3O_{40}]^{6-}$ and $[\alpha\text{-}1,2\text{-}PW_{10}V_2O_{40}]^{5-}$ were discussed, and also examined by the ^{31}P and ^{51}V NMR measurements.

The catalysis by $[\alpha\text{-}1,2\text{-}PW_{10}V_2O_{40}]^{5-}$ and $[\alpha\text{-}PMo_{11}VO_{40}]^{4-}$, and their stabilities as catalysts were strongly cation-dependent, i.e., the stabilities as catalysts of CH_3CN-soluble Bu_4N salts were superior to those of the water-soluble alkali metal salts. Since benzene hydroxylation by these polyoxometalates was accompanied with simultaneous decomposition of hydrogen peroxide, the significant effect of the used amounts of hydrogen peroxide was observed.

The reactions by the Keggin-type $[\alpha\text{-}1,4,9\text{-}PW_9V_3O_{40}]^{6-}$, the Dawson-type $[\alpha_2\text{-}1,2\text{-}P_2W_{16}V_2O_{62}]^{8-}$ and $[\alpha_2\text{-}P_2W_{15}Mo_2VO_{62}]^{7-}$ polyoxometalates showed approximately linear turnover vs. time curves without an induction period. Nevertheless, of particular note was the remarkable stability as catalyst observed in $[\alpha_2\text{-}P_2W_{15}Mo_2VO_{62}]^{7-}$. In this work, the reactions which occur on the vanadium species within the polyoxometalates have been found only by the precursors such as $K_6H[\alpha\text{-}1,2,3\text{-}SiW_9V_3O_{40}]$, $K_5[\alpha\text{-}1,2\text{-}PW_{10}V_2O_{40}]$ (only for the first reaction), $(Bu_4N)_4K[\alpha\text{-}1,2\text{-}PW_{10}V_2O_{40}]$, $(Bu_4N)_4[\alpha\text{-}PMo_{11}VO_{40}]$ and $K_8H[\alpha_2\text{-}P_2W_{15}Mo_2VO_{62}]$.

As a model reaction by the vanadium species generated from the polyoxometalates, examined was the benzene hydroxylation catalyzed by oligomeric and monomeric oxovanadium species present in the aqueous solutions, which were prepared by dissolving $NaVO_3$ or Na_3VO_4 in water with varied pH. The turnover vs. time curves were pH dependent. The ^{51}V NMR measurements have revealed that the $VO(O_2)^+$ or the $VO(O_2)_2^-$ species significantly contributed to the reaction.

Acknowledgements

Financial support by a Grant-in-Aid for Scientific Research (C) No. 10640552 from the Ministry of Education, Science and Culture, Japan is gratefully acknowledged.

References

[1] C.L. Hill, C.M. Prosser-McCartha, Coord. Chem. Rev. 143 (1995) 407.
[2] T. Okuhara, N. Mizuno, M. Misono, Adv. Catal. 41 (1996) 113.

[3] R. Neumann, Prog. Inorg. Chem. 47 (1998) 317.
[4] X. Wei, R.E. Bachman, M.T. Pope, J. Am. Chem. Soc. 120 (1998) 10248.
[5] K. Nomiya, H. Yanagibayashi, C. Nozaki, K. Kondoh, E. Hiramatsu, Y. Shimizu, J. Mol. Catal. A 114 (1996) 181.
[6] K. Nomiya, K. Yagishita, Y. Nemoto, T. Kamataki, J. Mol. Catal. A 126 (1997) 43.
[7] P.J. Domaille, J. Am. Chem. Soc. 106 (1984) 7677.
[8] R.G. Finke, C.A. Green, B. Rapko, Inorg. Synth. 27 (1990) 128.
[9] P.J. Domaille, Inorg. Synth. 27 (1990) 96.
[10] S.P. Harmalker, M.A. Leparulo, M.T. Pope, J. Am. Chem. Soc. 105 (1983) 4286.
[11] R.G. Finke, B. Rapko, R.J. Saxton, P.J. Domaille, J. Am. Chem. Soc. 108 (1986) 2947.
[12] P.J. Domaille, G. Watunya, Inorg. Chem. 25 (1986) 1239.
[13] M. Abbessi, R. Contant, R. Thouvenot, G. Herve, Inorg. Chem. 30 (1991) 1695.
[14] D. Rehder, Angew. Chem. Int. Ed. Engl. 30 (1991) 148.
[15] M. Aureliano, J. Leta, V.M.C. Madeira, L. de Meis, Biochem. Biophys. Res. Commun. 201 (1994) 155.
[16] J.J. Correia, L.D. Lipscomb, J.C. Dabrowiak, N. Isern, J. Zubieta, Arch. Biochem. Biophys. 309 (1994) 94.
[17] E. Heath, O.W. Howarth, J. Chem. Soc., Dalton Trans. (1981) 1105.
[18] S.E. O'Donnell, M.T. Pope, J. Chem. Soc., Dalton Trans., 1976, 2290.
[19] M.J. Clague, A. Butler, J. Am. Chem. Soc. 117 (1995) 3475.
[20] V. Conte, F. Di Furia, S. Moro, J. Mol. Catal. 104 (1995) 159.